

## VELOCITY EFFECTS ON THE BEHAVIOUR OF ASYMMETRICAL FRICTION CONNECTIONS (AFC)

**Jose C. Chanchi Golondrino\***, **Gregory A. MacRae\*\***, **J. Geoffrey Chase\*\***, **Geoffrey W. Rodgers\*\*** and **G. Charles Clifton\*\*\***

\* University of Canterbury - New Zealand, National University of Colombia - Colombia  
e-mail: jcchanchigo@unal.edu.co

\*\* University of Canterbury - New Zealand  
e-mail: gregory.macrae@canterbury.ac.nz, geoff.chase@canterbury.ac.nz, geoffrey.rodgers@canterbury.ac.nz

\*\*\* University of Auckland – New Zealand  
e-mail: c.clifton@auckland.ac.nz

**Keywords:** Asymmetrical Friction Connection, Velocity dependence, Low damage dissipaters, Energy dissipation, Shim materials

**Abstract.** *This paper reports on the hysteretic behaviour of Asymmetrical Friction Connection (AFC) assembled with different shim materials such as Aluminium, Brass, Mild Steel, Bisalloy 80, Bisalloy 400, and Bisalloy 500 subjected to a cyclic displacement regime applied with a quasi-static velocity of 10 mm/s and with higher velocities of 190mm/s. Results show that at the high velocity regardless of the shim material the hysteresis loop is less stable, and greater forces are required to activate the sliding mechanism of the slotted plate when compared with the hysteresis loop at the low velocity. Boundaries of the effective friction coefficient for the quasi-static and high velocity cases, as well as a model that represents the velocity dependence of AFCs in terms of the effective friction coefficient are presented.*

## 1 INTRODUCTION

### 1.1 Asymmetrical Friction Connections (AFC)

AFCs are a type of friction connection assembled with three steel plates and two thin plates termed shims. The three steel plates comprise a bottom plate termed fixed plate, a slotted plate located at the central part of the connection, and a top plate termed cap plate that is attached to the other two plates by means of high strength bolts. The shims are inserted at the interface slotted plate-fixed plate and at the interface slotted plate-cap plate creating a shear plane at each side of the slotted plate (Figure 1a). This type of connection can be used to dissipate seismic energy in different structural systems, and energy is dissipated when the slotted plate is forced to slide across the connection by overcoming the friction force generated at both sides of this plate as a result of the clamping force induced by the bolts on the connection. Quasi-static testing of this type of connection has shown that an almost square and stable hysteretic behaviour can be achieved by using shims with a hardness that is lower or greater than the hardness of the slotted plate (figure 1b). For instance the use of Aluminium, Brass, Bisalloy 400, or Bisalloy 500 shims was found to be suitable in terms of hysteretic behaviour of the connection when used on mild steel slotted plates (Chanchi et al. 2012). AFCs can be used as seismic dissipaters in different structural systems such as moment resistant frames (figure 1c) and braced frames (figure 1d). In moment resistant frames the AFC detail is placed at beam column joint where the energy is dissipated as the joint rotates (Clifton 2005), and in braced frames the AFC detail can be placed at one end of the brace where the energy is dissipated when the brace is elongated (Chanchi et al. 2014).

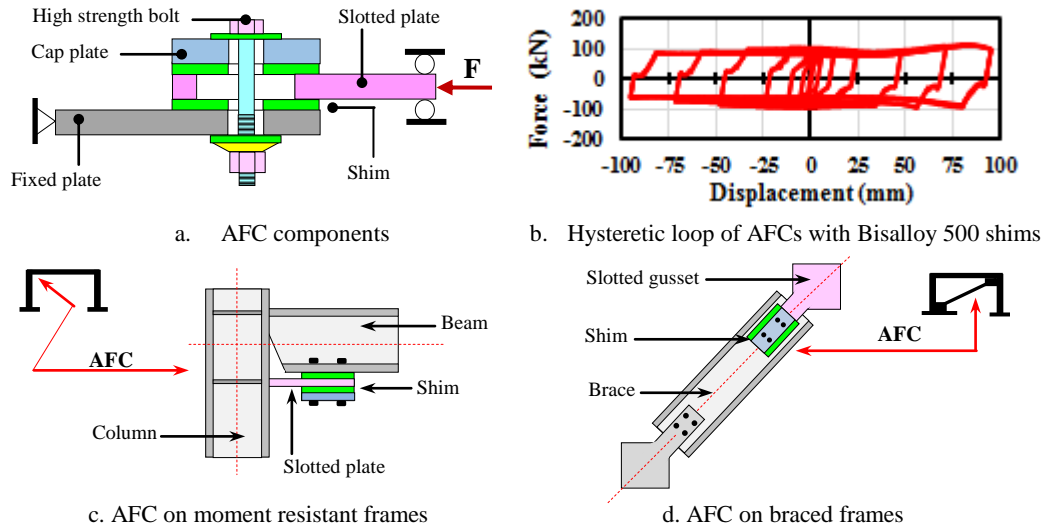


Figure 1. AFC components, hysteretic behaviour, and application

### 1.1 Research background

The concept of the AFC was proposed by Clifton 2005 when considering AFC subassemblies with brass shims tested in quasi-static conditions and over short sliding distances (i.e. up to 50mm). Results showed that by using dissimilar sliding surfaces the hysteretic behaviour of AFCs is stable and can be predicted using a bilinear hysteresis loop. MacRae et al. 2010 carried out quasi-static testing on beam-column joints equipped with AFC details assembled with Aluminium, Brass, and Mild Steel shims. Results confirmed the findings of Clifton 2005 regarding the stability of the hysteretic behaviour of the beam-column joint when using dissimilar sliding surfaces on the AFC detail. However, in the case of sliding Mild Steel slotted plates over Mild Steel shims (i.e. similar sliding surfaces) the behaviour of the beam-column joint was found to be stable when the sliding distances at the AFC detail were less than 50mm. Khoo et al. 2012 replicated the quasi-static testing carried out by Clifton 2005 on AFC subassemblies introducing the concept of using shims with greater hardness than the hardness of the slotted plate. Results showed that by sliding slotted plates of Mild Steel over Bisalloy 400 shims the hysteretic behaviour of the AFC subassemblies is very stable and with low degradation. Chanchi et al. 2012 tested quasi-statically AFC specimens with long slots (i.e. 200mm) with different shim materials such as Aluminium, Brass, Mild Steel, Bisalloy 80, Bisalloy 400, and Bisalloy 500. Results showed that a stable hysteretic behaviour of the AFCs can be achieved by either using shim materials with lower or greater hardness than the hardness of the slotted plate. Results also indicated that the use of Bisalloy 80 and Mild Steel shims on AFCs with Mild Steel slotted plates is not desirable because AFCs with this type of shims exhibited an unstable hysteretic behaviour when tested for sliding distances between 75 and 200mm. From the above research background it can be seen that the hysteretic behaviour of AFCs with different shim materials has been characterized in quasi-static conditions. However, there is no reference of research work quantifying the velocity dependence of AFCs when using different shim materials. For that reason, this paper compares the hysteretic behaviour at low and high velocities of AFCs using Aluminium, Brass, Mild Steel, Bisalloy 80, Bisalloy 400 and Bisalloy 500, and answers these questions:

- i) What are the effects of high velocities on the hysteresis loop of AFCs?
- ii) Does the velocity change the effective friction coefficient of AFCs?

- iii) What are the boundaries values of the effective friction coefficient of AFCs when considering the effect of the velocity?
- iv) What is a simple model for representing the effect of the velocity on the effective friction coefficients of AFCs?

## 2 MATERIALS

AFC specimens were assembled with a fixed, slotted and cap plates manufactured with Grade 300 Mild Steel plates of 20mm thickness, and shims of 6mm thickness manufactured with the materials specified in table 1. The shim materials were chosen in such a way that the ratio between the Brinell hardness of the shim material and the Brinell hardness of the slotted plate ( $\rho$ ) varied in the range 0.57 – 3.84 as shown in Table 1.

**Table 1.** Summary of materials used as shims

Material	Specification	Brinell Hardness (BH)	Hardness ratio $\rho$ ( )
Aluminium	5005GP Series Aluminium	75	0.58
Brass	UNS C26000 – ½ Hard Temper	82	0.63
Steel	Cold Rolled Mild Steel	130	1.00
Bisalloy 80	Bisplate 80	255	1.96
Bisalloy 400	Bisplate 400	400	3.08
Bisalloy 500	Bisplate 500	500	3.85

Two galvanized bolts of Grade 8.8 (i.e. 830 MPa ultimate strength) with 16mm diameter and 110mm length were used to clamp together the three steel plates and the two shims. The bolt assembly comprised a structural washer placed under the bolt head, a flat washer and a Belleville washer placed under the bolt nut. The threaded zone of the bolts was excluded from the two shear planes (Figure 2b). The AFC specimen was characterized by a slot of 200mm, a clamped zone of 180mm width and 290mm long with a grip length of 72mm, and two unclamped zones of 180mm width and 290mm long located at both sides of the clamped zone. At both ends of the AFC specimen six holes of 26mm diameter were drilled to attach the connection on testing rig (Figure 2a).

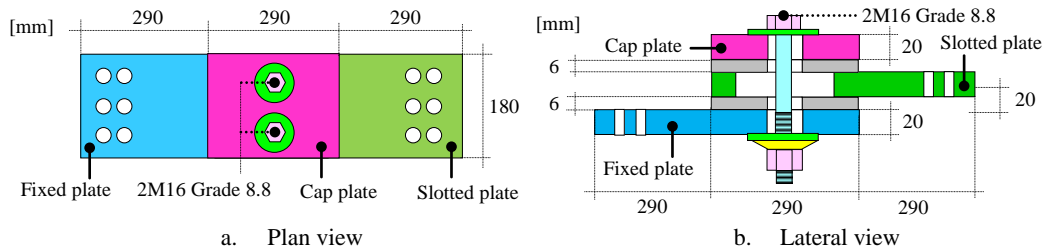
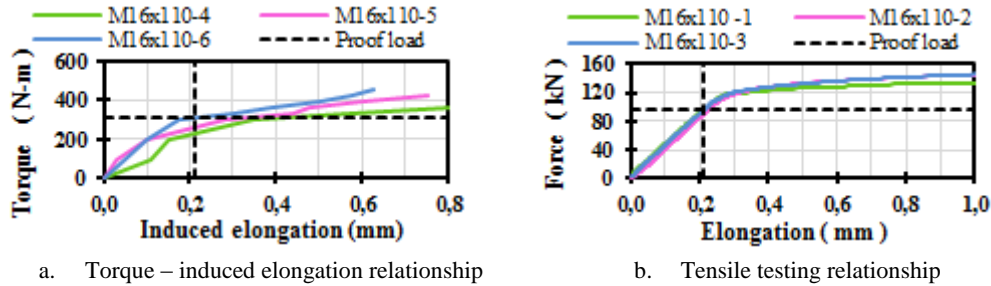


Figure 2. Configuration of an AFC specimen with 200mm slot and using two Grade 8.8 M16x110 bolts.

## 3 TESTING METHODS

### 3.1 AFC assembling procedure

Four AFC specimens were assembled at each type of shim material, so that a total of twenty four AFC specimens were considered in this research work. Each AFC specimen was assembled using the torque control method based on finding experimentally a torque that develops the proof load on the bolts (proof load torque).

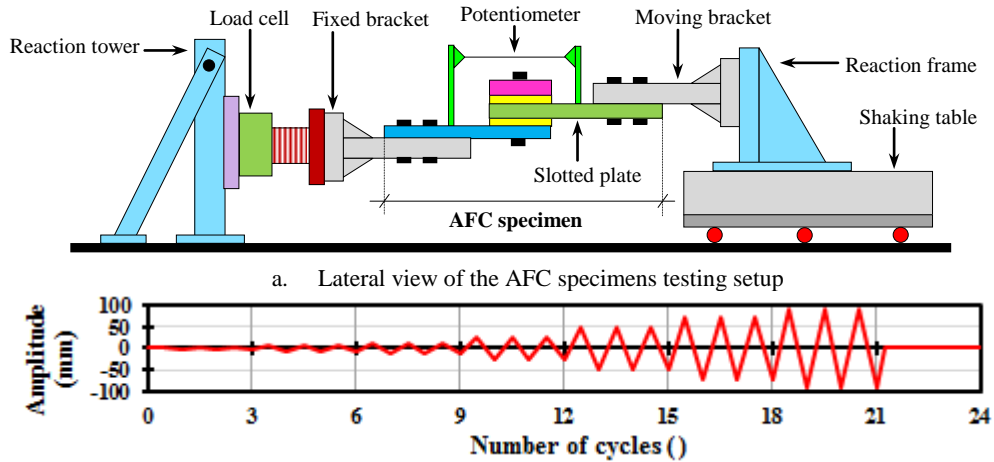


a. Torque – induced elongation relationship  
b. Tensile testing relationship  
Figure 3. Assembling relationships for an AFC specimen with two M16 110mm Grade 8.8 bolts.

The proof load torque was extrapolated from a relationship between torque and induced bolt elongation obtained from two bolts with a grip length equal to the grip length of the AFC specimens (i.e. 72mm). This torque – induced bolt elongation relationship was developed by gradually increasing the torque on the three bolts up to the failure torque, and by recording at each torque the elongation of the two bolts (Figure 3a). The bolt elongation used to extrapolate the assembling torque from the torque-induced bolt elongation relationship was defined as the elongation exhibited by three bolts when reaching the proof load on a tensile testing (Figure 3b). Using the above methodology a torque value of 300N-m from the finger tight condition was defined as proof load torque.

### 3.2 Testing setup

AFC specimens were tested in a setup horizontally arranged and constituted by a fixed and a moving support. The fixed support was assembled with a bracket bolted on a reaction frame and termed fixed bracket, and the moving support with a bracket attached to a frame bolted on a shaking table and termed moving bracket. Slip critical connections with six Grade 8.8 M24x120mm bolts were used to bolt the fixed and slotted plates of the AFC specimen onto the fixed and moving brackets of testing setup. By attaching the slotted plate onto the moving bracket, the shaking table was able to drive the slotted plate of the AFC specimen to target displacement and at pre-defined velocity (figure 4a).



a. Lateral view of the AFC specimens testing setup  
b. Displacement regime applied at constant velocities of 10 and 190 mm/s  
Figure 4. Testing setup and displacement regime used on the testing of AFC specimens.

This setup was instrumented with a load cell placed in series with the fixed bracket, and with one extensometer placed horizontally across the AFC specimen. Testing of AFC specimens was carried out by running the shaking table with a controlled displacement regime with a constant velocity. Half of the AFC specimens were tested by running the displacement regime at a constant quasi-static velocity of 10mm/s, and the other half of the specimens by running the displacement regime at a constant high velocity of 190mm/s. The displacement regime comprised 20 sawtooth cycles with amplitudes between 3 and 90% of the total slot length of the AFC specimen (i.e. 200mm) as shown in Figure 4b.

## 4 RESULTS AND ANALYSIS

### 4.1 Effects of the velocity on the hysteresis loop

Hysteresis loops recorded at quasi-static and high velocities (i.e. 10mm/s and 190mm/s) for AFCs assembled with different shim materials are presented in Figure 5.

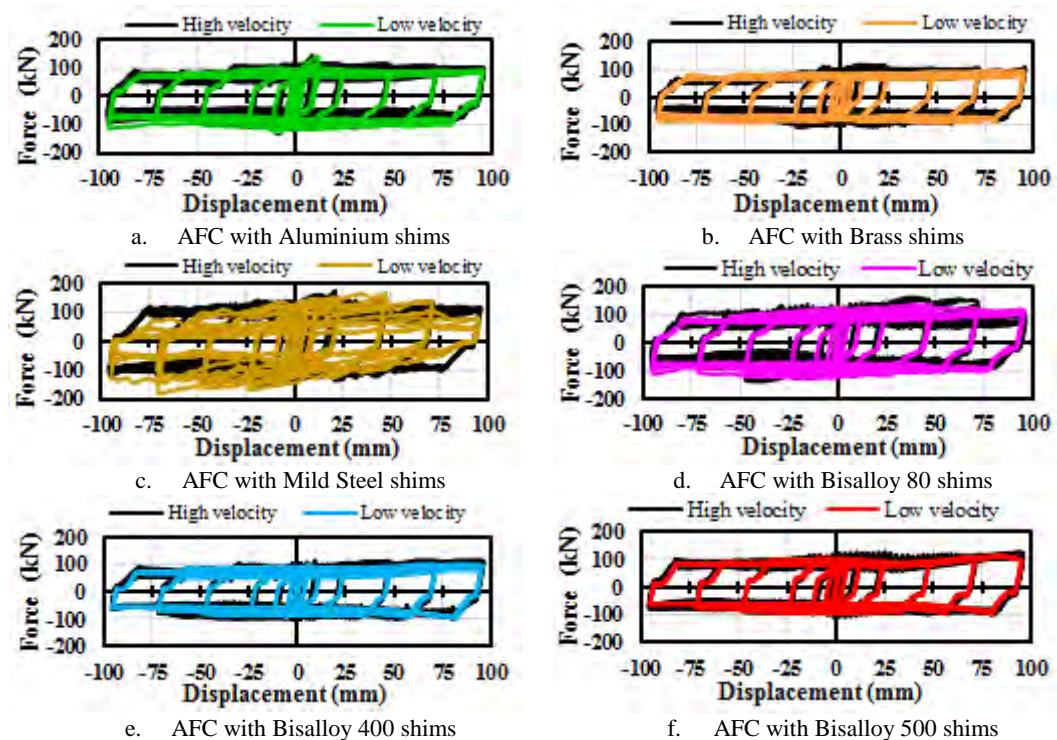


Figure 5. Hysteresis loop of AFCs with different shim materials

When comparing the hysteresis loops recorded at low and high velocities, two effects of increasing dramatically the testing velocity on the hysteresis loop can be observed: i) the post-yielding zone at high velocities is less stable than at low velocities (Figure 5), and ii) forces across the post-yielding at high velocities are greater than those recorded at low velocities. Both effects are more accentuated for shim materials with hardness similar to the hardness of the slotted plate (i.e. Mild Steel and Bisalloy 80 shims), rather than for shim materials where the shim hardness is either lower or greater than the hardness of the slotted plate. These two effects are linked to the development of an abrasive sliding mechanism where the

significant amount and size of the degraded particles degrading the sliding surfaces and observed at low velocities is significantly increased at high velocities.

#### 4.2 Effects of the velocity on the effective friction coefficient

The effective friction coefficient (Equation 1) was calculated as the ratio between the average force across the post-yielding zone of the hysteresis loop ( $F_{sliding}$ ) and the product of the number of bolts (i.e. 2), the number of shear planes (i.e. 2), and the bolt proof load (i.e. 95kN). Figure 6 presents the average effective friction coefficient from both loading directions calculated from two AFC specimens at each group of shims for the low and high velocity testing cases and at different sliding distances.

$$\mu_{effective} = \frac{F_{sliding}}{2 \times 2 \times 95} \quad (1)$$

In Figure 6 it can be seen that for all shim materials the effective friction coefficient at high velocity is greater than the effective friction coefficient at low velocity across the full sliding distance of the connection. It can also be seen that as the ratio between the hardness of the shim material and the hardness of the slotted plate material ( $\rho$ ) increases the effective friction coefficient at high velocities y closer to the effective friction coefficient at low velocities. This proximity between the effective friction coefficient at high and low velocities is attributed to adhesive sliding mechanisms typical of hardness ratios ( $\rho$ ) greater than 3 (Chanchi et al. 2012) where the amount and size of degraded particles is minor, so that as the degraded particles slide at high velocities there is minor increment on the friction force.

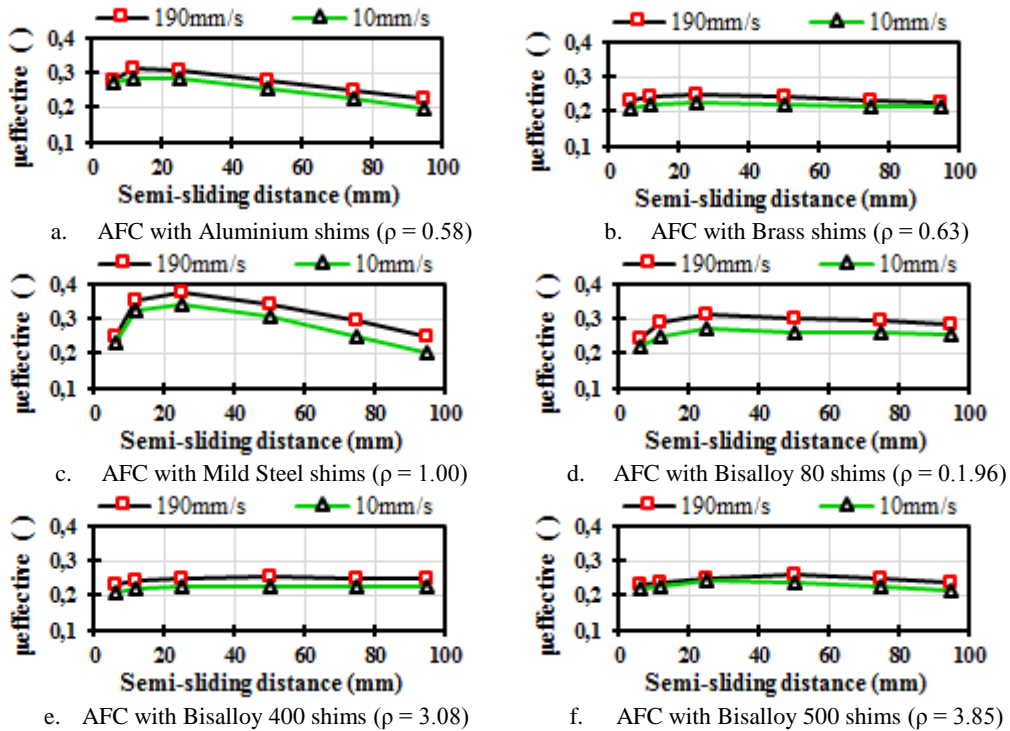


Figure 6. Effective friction coefficient ( $\mu_{effective}$ ) of AFCs with different shim materials.

#### 4.3 Effect of the shim hardness on the effective friction coefficient

The boundaries of the effective friction coefficient for low and high velocities for different shim materials were calculated as the average across the post-yielding zone from two AFC specimens at each testing velocity (Figure 7). Figure 7 shows that at low and high velocities the effective friction coefficient of AFC varies in the ranges 0.22 – 0.27 and 0.24 – 0.31 respectively.

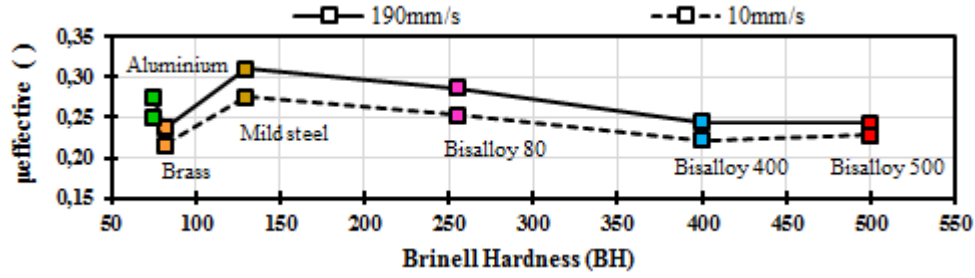


Figure 7. Effective friction coefficient ( $\mu_{\text{effective}}$ ) of AFCs with different shim material hardness.

Figure 7 also shows that the maximum effective friction coefficients with the greatest velocity dependence can be achieved by using hardness ratios of unity (i.e. Mild steel slotted plates sliding over Mild steel shims). However in this case the hysteretic behaviour of the AFC specimen is unstable. In contrast, minimum effective friction coefficients with the lowest velocity dependence and stable hysteretic behaviours can be achieved by using hardness ratios greater than 3.0 (i.e. Mild Steel slotted plates sliding over Bisalloy 400 or Bisalloy 500 shims).

#### 4.4 Velocity model

In order to quantify the velocity dependence of AFC specimens, they were assumed to behave as viscous dampers, where the force that activates the sliding of the connection ( $F$ ) is proportional to a coefficient that depends on the geometrical configuration of the connection ( $C$ ), to the testing velocity ( $V$ ), and to an exponent ( $\alpha$ ) that represents the magnitude of velocity dependence of the connection as shown in equation 2 (Peckan et al. 1995).

$$F = C \times V^\alpha \quad (2)$$

$$F_h = F_q \times \left[ \frac{V_h}{V_q} \right]^\alpha \quad (3)$$

$$\mu_h = \mu_q \times \left[ \frac{V_h}{V_q} \right]^\alpha \quad (4)$$

Using Equation 2 for both the quasi-static case (10mm/s) and the high velocity case (190mm/s), and equating the connection coefficient ( $C$ ), an expression that correlates the force at high velocity ( $F_h$ ), the force at quasi-static velocity ( $F_q$ ), the quasi-static velocity ( $V_q$ ), the high velocity ( $V_h$ ), and the velocity dependence exponent ( $\alpha$ ) was found (equation 3). This equation can be extended to the effective friction coefficient as shown in equation 4, and by using the boundaries of the effective friction coefficients found in section 4.3 the velocity dependence exponent ( $\alpha$ ) was quantified for different shim materials in figure 8. It can be seen that the velocity dependence exponent for AFC specimens varies in the range of 0.020 to



0.045 and the maximum and minimum values are presented for Mild Steel slotted plates sliding over Mild Steel shims and Bisalloy 400 or Bisalloy 500 shims respectively.

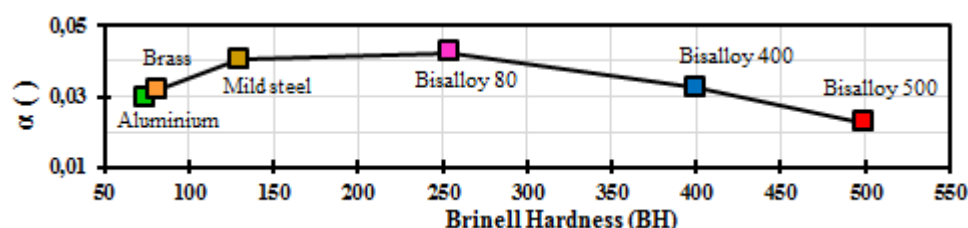


Figure 8. Velocity dependence exponent ( $\alpha$ ) of AFCs with different shim materials.

## 5 CONCLUSIONS

This paper describes the velocity effects on the AFC using different shim materials. It is shown that:

- i) At high velocities the hysteresis loop of AFCs loses stability, and greater forces are required to activate the sliding mechanism when compared with the forces required in quasi-static conditions.
- ii) The effective friction coefficient of AFCs increases with increments on the velocity. Magnitude of the increments on the effective friction coefficient depends on the ratio between the hardness of the shim material and the hardness of the slotted plate.
- iii) For ratios between the hardness of the shim material and the hardness of the slotted plate (hardness ratio) varying on the range 0.58-3.85, the effective friction at low and high velocities vary in the ranges 0.22-0.27 and 0.24-0.31 respectively.
- iv) The effective friction coefficient at high velocities can be quantified as the product between the effective friction coefficient at low velocities and the ratio between the high and low velocity raised to the power of an exponent that varies in the range of 0.020 - 0.045.

## REFERENCES

- [1] Chanchi, J.C., MacRae, G.A., Chase, G., Rodgers, G., and Clifton, C. (2012). Behaviour of asymmetrical friction connections using different shim materials. *New Zealand Society for Earthquake Engineering Conference*.
- [2] Clifton, G.C. (2005). Semi-Rigid Joints for Moments Resisting Steel Framed Seismic Resisting Systems. *Published PhD Thesis, Department of Civil and Environmental Engineering*. University of Auckland – New Zealand.
- [3] Chanchi, J.C., Xie R., MacRae, G.A., Chase, G., Rodgers, G., and Clifton, C. (2014). Low damage brace using Asymmetrical Friction Connections. *New Zealand Society for Earthquake Engineering Conference*.
- [4] MacRae, G.A., Clifton, C.G., MacKinven, H., Mago, N., Butterworth, J., Pampanin, S. (2010). The Sliding Hinge Joint Moment Connection. *Bulletin of the New Zealand Society for Earthquake Engineering*.
- [5] Khoo, H.H., Clifton, C., Butterworth, J., MacRae, G. and Ferguson, G. (2011) Influence of steel shimhardness on the Sliding Hinge Joint. *Journal of Constructional Steel Research*.
- [6] Pekcan, G., Mander, J. B., M. Eeri, and Chen, S. S. (1995). The Seismic Response of a 1:3 Scale Model R.C. Structure with Elastomeric Spring Dampers. *Earthquake Spectra*, Vol. 11, No. 2, pp 249 – 267.